Nuclear structure studies with (e,e'), (π,π'), and (γ,π) reactions: Applications to ^{10}B

T. Sato, N. Odagawa, and H. Ohtsubo
Department of Physics, Osaka University, Toyonaka, Osaka 560, Japan

T.-S. H. Lee
Physics Division, Argonne National Laboratory, Argonne, Illinois 60439
(Received 1 October 1993)

Theoretical approaches for investigating nuclear structure with (e,e') (π,π'), and (γ,π) reactions are presented and applied to study the shell-model description of ^{10}B. The distorted-wave impulse approximation formulated in momentum space is used to calculate the cross sections of (π,π') and (γ,π) reactions from the $\pi N \to \pi N$ and $\pi N \to \gamma N$ off-shell amplitudes which are generated from the model of Nozawa, Blankleider, and Lee [Nucl. Phys. **A513**, 459 (1990)]. It is found that the nonlocal effects due to πN off-shell dynamics and nucleon Fermi motion are important in predicting (γ,π) cross sections. The one-pion-exchange two-body exchange currents are included in (e,e') calculations. It is shown that the core polarization effects, calculated in a perturbation approach including excitations up to $6\hbar\omega$, are essential in obtaining quantitative agreements with the data with no adjustable parameters. The predictions based on the shell model of Cohen and Kurath [Nucl. Phys. **73**, 1 (1965)] and Hague and Maripuu [Phys. Rev. C **8**, 1609 (1973)] are compared in order to illustrate the use of (e,e'), (π,π'), and (γ,π) reactions in distinguishing nuclear structure theories which are almost equivalent in describing static properties of nuclei. Predictions for future (e,e') and (γ,π) experiments are also presented.

PACS number(s): 21.60.Cs, 25.30.Dh, 25.80.Ek, 27.20.+n

I. INTRODUCTION

It has been well recognized that pions and electrons are complementary to each other in probing the structure of nuclei. The study of electron scattering has provided important information about the electromagnetic currents inside the nucleus. By combining it with the study of pion scattering in the Δ region, the relative importance between the proton and neutron excitations has been probed very effectively. A natural extension of these efforts is to also investigate pion photoproduction reaction, which has certain unique features. For example, the charged pion photoproduction, which is dominated by the Kroll-Ruderman term $(\boldsymbol{\sigma}\cdot\boldsymbol{\epsilon})$ at low energies, is far more effective than electron scattering and pion scattering in probing nuclear spin-isospin response. The usefulness of a study of both the (e,e') and (γ,π) reactions in investigating nuclear structure has been demonstrated, for example, by Sato, Koshigiri and Ohtsubo [4]. Obviously, the most fruitful approach to study nuclear structure is to carry out a simultaneous study of (e,e'), (π,π'), and (γ,π) reactions. This type of study is possible for the $1p$-shell nuclei, owing to the existence of extensive (e,e') and (π,π') data and the possibility of carrying out precision measurements of (γ,π) reactions in the near future at several electron facilities. The objective of this work is to develop theoretical approaches for pursuing such a study.

We adopt the well-developed formulations [5] to carry out (e,e') studies. The calculations include the one-pion-exchange currents derived in Ref. [4]. Following the previous works, we assume that the (π,π') and (γ,π) reaction can be described by the distorted-wave-impulse approximation (DWIA). The scattering amplitudes are then expressed in terms of pion wave functions, off-shell scattering t matrix on a nucleon bound inside the nucleus, and one-body nuclear transition densities. To account for the nonlocal effects due to the off-shell t matrix and relativistic kinematics associated with nuclear Fermi motion, calculations for both the (π,π') and (γ,π) are carried out in momentum space. For (π,π') calculations, we therefore follow the momentum-space DWIA formulation developed in Refs. [6,7].

The majority of the existing DWIA calculations [8–13] of exclusive (γ,π) reactions were performed by using the photoproduction operators developed by Blomqvist and Laget [14]. Although the model has made important contributions to the field, there are some theoretical questions concerning its dynamical content. In particular, the nondelta term of the Blomqvist and Laget model is not unitary. Furthermore, the model does not dynamically define the off-shell behavior of the elementary $\gamma N \to \pi N$ process occurring inside the nucleus. The importance of off-shell dynamics in relating the nuclear structure to intermediate energy nuclear reactions has been stressed extensively in the literature. The advance made by Nozawa, Blankleider, and Lee (NBL) [1] was to provide a dynamical model for generating off-shell dynamics of the $\gamma N \to \pi N$ process within the constraints of unitarity and gauge invariance. The main effort of this work is to develop an approach to incorporate the NBL model in the DWIA study of (γ,π) reaction.

It is necessary to briefly describe the NBL model in order to indicate the main feature of our DWIA formu-

lation of the (γ,π) reaction. The model is defined within a Hamiltonian formulation with the assumption that the basic degrees of freedom of πN and γN systems are π, N, Δ, and the electromagnetic field. The model Hamiltonian is written as

$$H = H_0 + H_I + \int d\mathbf{x}\, J_\mu(\mathbf{x}) A^\mu(\mathbf{x}), \tag{1}$$

where H_0 is a free energy operator, H_I describes relevant hadronic interactions in terms of vertex interactions $\pi N \leftrightarrow N$ and $\Delta \leftrightarrow \pi N$, and a πN separable potential. They are determined from fitting the πN scattering phase shifts. The last term of the above equation defines the electromagnetic interaction in terms of electromagnetic field A^μ and current operator J^μ. By employing the standard scattering theory, the current matrix element of the $\gamma N \to \pi N$ process in the center-of-mass frame takes the following form:

$$J_\mu(\mathbf{Q},\boldsymbol{\kappa},W) = \langle \mathbf{Q}|J_\mu|\boldsymbol{\kappa}\rangle + \int d\mathbf{Q}' \frac{T_{\pi N,\pi N}(\mathbf{Q},\mathbf{Q}',W)\langle \mathbf{Q}'|J_\mu|\boldsymbol{\kappa}\rangle}{W - e(\mathbf{Q}') - \omega_\pi(\mathbf{Q}') + i\epsilon}, \tag{2}$$

where $\mathbf{Q}$ and $\boldsymbol{\kappa}$ are, respectively, the πN and γN relative momenta, $e(\mathbf{Q}) = (\mathbf{Q}^2 + m_N^2)^{1/2}$ is the nucleon energy, and $\omega_\pi(\mathbf{Q}) = (\mathbf{Q}^2 + m_\pi^2)^{1/2}$ is the pion energy. The second term of Eq. (2) describes the effect due to πN final-state interactions. It is determined by the off-shell matrix element of the πN scattering t matrix, which can be calculated from the hadronic part of the Hamiltonian $H_0 + H_I$ by solving πN scattering equations. The plane-wave matrix elements of the current operator in the right-hand side of Eq. (2) are defined by the low-order Feynman amplitudes illustrated in Fig. 1:

$$\langle \mathbf{Q}|J_\mu|\boldsymbol{\kappa}\rangle = \langle \mathbf{Q}|J_\mu^{\text{Born}}|\boldsymbol{\kappa}\rangle + \langle \mathbf{Q}|J_\mu^{\Delta}|\boldsymbol{\kappa}\rangle, \tag{3}$$

where

$$\langle \mathbf{Q}|J_\mu^{\text{Born}}|\boldsymbol{\kappa}\rangle = [\text{Figs. 1(a)} - \text{1(f)}] \times F_{\text{cut}}(\mathbf{Q}), \tag{4}$$

is called the Born term (nonresonant term). The second term of Eq. (3) describes the Δ excitation, as illustrated in Fig. 1(g). A cutoff function $F_{\text{cut}}(\mathbf{Q}) = \Lambda^2/(\Lambda^2 + \mathbf{Q}^2)$ has been introduced to make the Born term a square integrable function. The model defined above is gauge invariant and unitary, as was discussed in detail in Ref. [1]. The parameters of the Born term are taken from the literature. The only adjustable parameters of the model are the cutoff Λ for the Born terms, the magnetic $M1$ $[G_M(0)]$ and electric $E2$ $[G_E(0)]$ transitions of the $\gamma N \leftrightarrow \Delta$ excitation. It was found that the data of $\gamma N \to \pi N$ up to about $E_\gamma = 400$ MeV can be best reproduced with $\Lambda = 650$ MeV/c, $G_M(0) = 2.28$, and $G_E(0) = 0.07$.

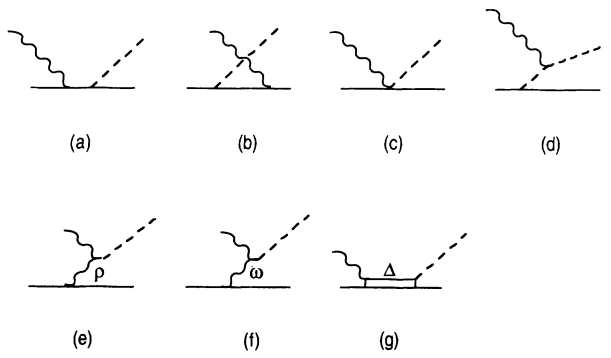

FIG. 1. The $\gamma N \to \pi N$ mechanisms of NBL model [1].

An important point to note is that within the Hamiltonian formulation, the off-shell current matrix elements with $W \neq e(\mathbf{Q}) + \omega_\pi(\mathbf{Q}) \neq e(\boldsymbol{\kappa}) + \kappa$ are well defined theoretically by Eq. (2). This is not the case for the model of Blomqvist and Laget [14], and the models based on dispersion relations or K-matrix method [11]. We will see in Sec. III that the DWIA amplitude of pion photoproduction on nuclei is determined by off-shell amplitudes of $\gamma N \to \pi N$ process. The use of the NBL model clearly makes our approach significantly different from all previous works.

As a first step, it is necessary to test the accuracy of our approach in a region where nuclear structure is nontrivial but can be described by well-developed nuclear theories. We therefore consider the $1p$-shell nuclei to which extensive works based on the shell model of Cohen and Kurath [2] have been carried out. With the single-particle energies and the residual interactions within the $1p$ shell determined by fitting the low-lying nuclear energy levels, the model of Cohen and Kurath describes very well the magnetic moments, magnetic dipole transitions, and Gamma-Teller matrix elements. To describe the transitions at large momentum transfer and higher multipoles, it is necessary to take into account the configurations outside the $1p$ shell. This is done in this work by calculating core polarization effects using the perturbation theory. This approach has been established in the studies of electron scattering, muon capture, and beta decay [4,15–18], and is known to be very different from the commonly used procedures of introducing enhancement factors for the bare transition operators. We will see that the core polarization effect plays an important role in obtaining agreements with the data with no adjustable parameters in our calculations.

An interesting question to ask is the following: To what extent can a simultaneous study of (e,e'), (π,π'), and (γ,π), reactions distinguish different nuclear models? To explore this, we also consider the shell model of Hauge and Maripuu [3]. They used the Sussex effective interactions [19] deduced from nucleon-nucleon phase shifts. The energies and the range parameter b of the assumed harmonic-oscillator wave functions are adjusted to reproduce the low-lying energy levels. They also succeeded in explaining the low-lying properties of $1p$-shell nuclei mentioned above. Therefore, it is very interesting to compare the predictions from this shell model with that from the model of Cohen and Kurath.

In this paper, we focus our study on ^{10}B, which is the most complex nucleus in the $1p$-shell region and has been extensively studied both experimentally and theoretically. Our investigations of other $1p$-shell nuclei will be published elsewhere.

In Sec. II, we briefly recall the essential formulas for calculating (e,e') and (π,π') scattering. A momentum-space DWIA formulation of the (γ,π) reaction is presented in Sec. III. In Sec. IV, the perturbative calculation of core polarization effects in nuclear excitations is outlined. The results and discussions are presented in Sec. V.

II. FORMULATIONS OF ELECTRON SCATTERING AND PION SCATTERING

The formulations for calculating the cross sections of electron scattering and pion scattering have been developed, respectively, in Refs. [5,7]. We therefore only recall formulas necessary for defining notations and indicating the nuclear structure input to the calculations of these two processes.

A. Electron scattering

The quantities of interest are the charge $F_C(q)$ and transverse $F_T(q)$ form factors defined as follows:

$$F_C^2(q) = \sum_J |C_J(q)|^2, \tag{5}$$

$$F_T^2(q) = \sum_J (|T_J^E(q)|^2 + |T_J^M(q)|^2) \tag{6}$$

with

$$C_J(q) = \langle J_f||\hat{C}_J(q)||J_i\rangle, \tag{7}$$

$$T_J^E(q) = \langle J_f||\hat{T}_J^E(q)||J_i\rangle, \tag{8}$$

$$T_J^M(q) = \langle J_f||\hat{T}_J^M(q)||J_i\rangle, \tag{9}$$

where $|J_i\rangle$ and $|J_f\rangle$ are, respectively, the initial and final nuclear state vectors. $q^\mu = (\omega,\mathbf{q})$ is the four momentum transfer to the nucleus. $\hat{C}_J$, $\hat{T}_J^E$, and $\hat{T}_J^M$ are, respectively, the Coulomb, electric, and magnetic multipole operators with rank J and parity change $(-1)^J$, $(-1)^J$, and $(-1)^{(J+1)}$. They are defined in terms of nuclear charge density operator $\rho(\mathbf{x})$ and current density operator $\mathbf{J}(\mathbf{x})$

$$\hat{C}_{JM}(q) = \int j_J(qx) Y_{JM}(\hat{x}) \rho(\mathbf{x}) d\mathbf{x}, \tag{10}$$

$$\hat{T}_{JM}^E(q) = \frac{1}{q}\int \{\nabla \times [j_J(qx)\mathbf{Y}_{JJ1}^M(\hat{x})]\}\cdot \mathbf{J}(\mathbf{x}) d\mathbf{x}, \tag{11}$$

$$\hat{T}_{JM}^M(q) = \int j_J(qx)\mathbf{Y}_{JJ1}^M(\hat{x})\cdot \mathbf{J}(\mathbf{x}) d\mathbf{x}. \tag{12}$$

The currents included in our calculations are

$$\rho(\mathbf{x}) = \rho^{(1)}(\mathbf{x}) \tag{13}$$

and

$$\mathbf{J}(\mathbf{x}) = \mathbf{J}^{(1)}(\mathbf{x}) + \mathbf{J}^{(2)}(\mathbf{x}), \tag{14}$$

where the one-body currents $(\rho^{(1)},\mathbf{J}^{(1)})$ are of the usual nonrelativistic forms, the two-body spatial part $\mathbf{J}^{(2)}$ is the static one-pion-exchange current. Explicit expressions of these currents are given in Ref. [4]. To ensure that the electric form factor has a correct low momentum transfer behavior, we use the current conservation relation to rewrite the electric form factor $T_J^E(q)$ as

$$T_{JM}^E(q) = -\frac{\omega}{q}\sqrt{\frac{J+1}{J}}C_J(q) - i\sqrt{\frac{2J+1}{J}}\left\langle J_f\left|\left|\int j_{J+1}(qx)\mathbf{Y}_{JJ+11}^M(\hat{x})\cdot\mathbf{J}(\mathbf{x})d\mathbf{x}\right|\right|J_i\right\rangle. \tag{15}$$

In the $q\to 0$ limit, the second term vanishes and Eq. (15) is reduced to the Siegert theorem. This extension of Siegert's theorem to the high momentum-transfer region was discussed in Ref. [4].

With the above definitions, it is straightforward to calculate charge and transverse form factors from shell-model wave functions. For the calculation of one-body current contributions, the nuclear structure input is the one-body transition matrix defined as

$$A_{J(LS)}^{\alpha,\beta}(J_f,J_i) = \langle J_f||\left(a_\alpha^+\otimes\tilde{a}_\beta\right)_J||J_i\rangle(\hat{j}_\alpha\hat{j}_\beta\hat{L}\hat{S})^{1/2} \times \begin{Bmatrix} l_\alpha & \frac{1}{2} & j_\alpha \\ l_\beta & \frac{1}{2} & j_\beta \\ L & S & J \end{Bmatrix}, \tag{16}$$

where $\hat{j} = 2j+1$, $\tilde{a}_\beta = (-1)^{j_\beta - m_\beta}a_{j_\beta,-m_\beta}$, and α and β collectively denote the single-particle quantum numbers: $n_\alpha(l_\alpha 1/2)j_\alpha$. a_α^+ and a_β are, respectively, the creation and annihilation operators for the single-particle state. For example, the $E2$ transition is calculated from $A_{2(20)}^{\alpha,\beta}(J_f,J_i)$. The calculation of two-body current contributions requires two-body transition density matrices. It is not relevant to the discussions in this paper and hence is not presented here.

B. Pion inelastic scattering

Within the momentum-space DWIA formulation developed in Refs. [6,7], the (π,π') cross section is calculated from pion wave functions, $\pi N\to\pi N$ off-shell t matrix and nuclear one-body transition density. As derived in Ref. [7], the (π,π') scattering amplitude in the π-nucleus center-of-mass frame can be written in the following partial-wave form

$$T_{f,i} = \langle J_f, M_f, \pi(\mathbf{q}'_A)|T|J_i, M_i, \pi(\mathbf{q}_A)\rangle$$
$$= \sum_{L'M'LMJ} (\hat{L}\hat{L}'\hat{J}_f)^{1/2} Y^*_{L'M'}(\hat{q}'_A) Y_{LM}(\hat{q}_A)$$
$$\times (-1)^{J_f - M_f + M'} \begin{pmatrix} L & L' & J \\ -M & M' & M_i - M_f \end{pmatrix} \begin{pmatrix} J & J_i & J_f \\ M_f - M_i & M_i & M_f \end{pmatrix}$$
$$\times \int_0^\infty q'^2 dq' \int_0^\infty q^2 dq\, \chi^{(-)*}_{L'q'_A}(q') U^{fiJ}_{L'L}(q', q) \chi^{(+)}_{Lq_A}(q), \tag{17}$$

where $\mathbf{q}$ is the pion-nucleus relative momentum and $\chi^{(\pm)}_{Lq_A}(q)$ is the pion wave function of angular momentum L. The nuclear excitation is described by the transition potential which can be decomposed into products of two parts

$$U^{fiJ}_{L'L}(q', q) = \sum_{l'lKS} I^{fiJ}_{l'lKS}(q', q) H^{L'LJ}_{l'lKS}(q', q). \tag{18}$$

The nuclear structure information is contained in the first term of the above equation

$$I^{fiJ}_{l'lKS}(q', q) = \int_0^\infty j_{l'}(q'r) F^{fiJ}_{KS}(r) j_l(qr) r^2 dr. \tag{19}$$

Within the nuclear shell model, the nuclear transition density F^{fiJ}_{KS} is defined as

$$F^{fiJ}_{KS}(r) = \sum_{\alpha,\beta} \langle J_f||[a^\dagger_\alpha \otimes \tilde{a}_\beta]_J||J_i\rangle$$
$$\times (4\pi\hat{j}_\alpha)^{1/2} \langle \alpha|||[Y_K(\hat{r}) \otimes \sigma_S]_J|||\beta\rangle$$
$$\times R_{n_\alpha l_\alpha}(r) R_{n_\beta l_\beta}(r). \tag{20}$$

We now note that the above equation and Eq. (16) for electron scattering are determined by the same one-body matrix element

$$\langle J_f||[a^\dagger_\alpha \otimes \tilde{a}_\beta]_J||J_i\rangle.$$

This establishes the connection between (e,e') and (π,π') scattering. The reaction dynamics is determined by the πN off-shell t matrix

$$H^{L'LJ}_{l'lKS}(q', q) = i^{l'-l} (\hat{K})^{1/2} \hat{l}\hat{l}' \begin{pmatrix} l & l' & K \\ 0 & 0 & 0 \end{pmatrix}$$
$$\times \sum_\lambda (\hat{\lambda})^{3/2} (-1)^{\lambda - J} \begin{pmatrix} L' & l' & \lambda \\ 0 & 0 & 0 \end{pmatrix} \begin{pmatrix} L & l & \lambda \\ 0 & 0 & 0 \end{pmatrix} \begin{Bmatrix} L & L' & J \\ \lambda & \lambda & S \\ l & l' & K \end{Bmatrix} t^\lambda_S(q', q, W_0), \tag{21}$$

where t^λ_0 and t^λ_1 are, respectively, the spin-independent and spin-dependent parts of the πN off-shell t matrix with an orbital angular momentum λ. The procedure of Ref. [20] is used to calculate $t^\lambda_S(q', q, W)$ from a πN potential model. It involves the transformation from a πN center-of-mass frame to a π nucleus center-of-mass frame. A similar procedure will be used in our later DWIA formulation of the (γ,π) reaction.

The only differences between the present (π,π') calculations and that of Ref. [7] are in using the NBL model to generate the $\pi N \to \pi N$ off-shell t matrix $t^\lambda_S(q', q, W)$ and using more accurate optical potentials to calculate pion wave functions. At low pion energies, we use the model developed by Carr, McManus, and Stricker-Bauer [21]. At Δ resonance energies, the optical potential derived from the Δ-hole model [22] is used. Each model was developed to describe not only elastic scattering cross sections, but also the reaction cross sections. This is very essential in obtaining accurate pion wave functions in the region where nuclear transitions take place. Unfortunately, each model emphasized a different energy region and we are forced to have this inconsistency in the present calculations. This should be improved in the near future. Except for the (γ,π) calculations at energies below 200 MeV, the pion optical potential of the Δ-hole model is used in all of the calculations presented in Sec. V.

III. THE DWIA FORMULATION OF (γ,π) REACTION

Following the previous investigations [4,8–13], we assume that the (γ,π) reaction can also be described by DWIA. In the projectile-nucleus center-of-mass system (ACM), the transition amplitude for an incident photon with momentum $\mathbf{k}_A$ and helicity λ is of the following form:

$$T_f i = \langle J_f M_f, \pi(\mathbf{q}_A)|T|J_i M_i, \gamma(\mathbf{k}_A, \lambda)\rangle$$
$$= \sum_{\alpha,\beta} \sum_{m_i, m_f} \int d\mathbf{q}\, d\mathbf{p}_i d\mathbf{p}_f \delta(\mathbf{p}_f + \mathbf{q} - \mathbf{p}_i - \mathbf{k}_A) \psi^*_\alpha(\mathbf{p}_f, m_f) \psi_\beta(\mathbf{p}_i, m_i)$$
$$\times \chi^{(-)*}_{\mathbf{q}_A}(\mathbf{q}) t^{\gamma,\pi}_{m_f,m_i}(\mathbf{p}_f, \mathbf{q}; \mathbf{p}_i, \mathbf{k}_A, \epsilon_\lambda, W_A) \langle J_f|a^\dagger_\alpha a_\beta|J_i\rangle, \tag{22}$$

where $\mathbf{q}$ is the pion momentum, $\mathbf{p}_i$ and $\mathbf{p}_f$ are nucleon momenta, m_i and m_f are z components of nucleon spin, $\chi^{(-)*}_{\mathbf{q}_A}(\mathbf{q})$ is the pion scattering wave function, and $\psi_\alpha(\mathbf{p}, m)$ is the shell-model single-particle wave function. The matrix element

$$t^{\gamma,\pi}_{m_f,m_i}(\mathbf{p}_f, \mathbf{q}; \mathbf{p}_i, \mathbf{k}_A, \epsilon_\lambda, W_A)$$

is the off-shell scattering amplitude of the

$$\gamma(\mathbf{k}_A, \epsilon_\lambda) + N(\mathbf{p}_i, m_i) \to \pi(\mathbf{q}) + N(\mathbf{p}_f, m_f)$$

reaction, as illustrated in Fig. 2. Within the NBL model (or any model with πN scattering described by a potential), it is necessary to first evaluate the $\gamma N \to \pi N$ amplitude in the pion-nucleon center-of-mass frame (2CM), as defined by Eq. (2). The amplitude needed in evaluating Eq. (22) in the ACM system is obtained by using the procedure developed in the study of pion-nucleus scattering [20]. In addition, we also have to consider the Lorentz transformation of current operators. Explicitly, we have

$$t^{\gamma,\pi}_{m_f m_i}(\mathbf{p}_f, \mathbf{q}; \mathbf{p}_i, \mathbf{k}_A, \epsilon_\lambda, W_A)$$

$$= F^{1/2}(\mathbf{Q}, \mathbf{p}_f, \mathbf{q}, \boldsymbol{\kappa}, \mathbf{k}_A, \mathbf{p}_i) \times \langle m_f | \boldsymbol{\epsilon}_\lambda \cdot \mathbf{J}_A(\mathbf{Q}, \boldsymbol{\kappa}, W_A) | m_i \rangle \tag{23}$$

with

$$F(\mathbf{Q}, \mathbf{p}_f, \mathbf{q}, \boldsymbol{\kappa}, \mathbf{k}_A, \mathbf{p}_i) = \frac{e(\mathbf{Q})\omega_\pi(\mathbf{Q})}{e(\mathbf{p}_f)\omega_\pi(\mathbf{q})} \frac{\kappa e(\boldsymbol{\kappa})}{k_A e(\mathbf{p}_i)} , \tag{24}$$

where $e(\mathbf{p}) = \sqrt{m_N^2 + \mathbf{p}^2}$ is the nucleon energy and $\omega_\pi(\mathbf{q}) = \sqrt{m_\pi^2 + \mathbf{q}^2}$ is the pion energy. The relative momenta $\mathbf{Q}$ for the πN state and $\boldsymbol{\kappa}$ for the γN state are evaluated from individual momenta $\mathbf{p}_i$, $\mathbf{p}_f$, $\mathbf{q}$, and $\mathbf{k}_A$ in ACM by using appropriate Lorentz transformations. Explicitly, we have

$$\mathbf{Q} = \left(\mathbf{q} - \frac{\omega_\pi}{\sqrt{S_\pi}} \mathbf{P} \right) + \frac{W_\pi - \sqrt{S_\pi}}{\sqrt{S_\pi}} (\mathbf{q} \cdot \hat{P}) \hat{P} ,$$

$$\boldsymbol{\kappa} = \left(\mathbf{k}_A - \frac{k_A}{\sqrt{S_\gamma}} \mathbf{P} \right) + \frac{W_\gamma - \sqrt{S_\gamma}}{\sqrt{S_\gamma}} (\mathbf{k}_A \cdot \hat{P}) \hat{P} \tag{25}$$

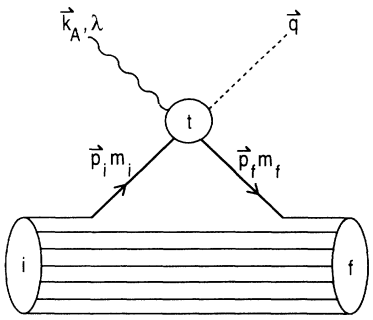

FIG. 2. Graphical representation of the (γ, π) reaction within the distorted-wave impulse approximation.

with

$$\mathbf{P} = \mathbf{p}_i + \mathbf{k}_A = \mathbf{p}_f + \mathbf{q} ,$$
$$W_\pi = e(\mathbf{p}_f) + \omega_\pi(\mathbf{q}), \quad W_\gamma = e(\mathbf{p}_i) + k_A , \tag{26}$$
$$S_\pi = W_\pi^2 - \mathbf{P}^2, \quad S_\gamma = W_\gamma^2 - \mathbf{P}^2 .$$

In the limit where the total π-nucleon momentum is small, the expressions of Eq. (25) are reduced to the form commonly used in π-nucleus scattering [20]

$$\mathbf{Q} \to \frac{e(\mathbf{p}_f)\mathbf{q} - \omega_\pi(\mathbf{q})\mathbf{p}_f}{e(\mathbf{p}_f) + \omega_\pi(\mathbf{q})} ,$$
$$\boldsymbol{\kappa} \to \frac{e(\mathbf{p}_i)\mathbf{k}_A - k_A \mathbf{p}_i}{e(\mathbf{p}_i) + k_A} . \tag{27}$$

In the Δ-hole model calculations of (γ, π) reactions [23], one further takes static limit $e(\mathbf{p}) \to m_N$ to simplify the calculation. In this work, we use Eqs. (24)–(26).

In Eq. (23), the current operator $\mathbf{J}_A$ in the ACM is related to the current $\mathbf{J}$ operator in 2CM by a Lorentz transformation. Its matrix element can therefore be calculated from the matrix elements of $\mathbf{J}$ defined by Eq. (2). We find that

$$\mathbf{J}_A(\mathbf{Q}, \boldsymbol{\kappa}, W_A)$$

$$= \mathbf{J}(\mathbf{Q}, \boldsymbol{\kappa}, W) + \frac{\mathbf{P}}{\sqrt{S_\gamma}} \left(J_0(\mathbf{Q}, \boldsymbol{\kappa}, W) + \frac{\mathbf{J}(\mathbf{Q}, \boldsymbol{\kappa}, W) \cdot \mathbf{P}}{W_\gamma + \sqrt{S_\gamma}} \right) , \tag{28}$$

where $W = (W_A^2 - \mathbf{P}^2)^{1/2}$. The time component J_0 in the above equation can be expressed in terms of the spatial component $\mathbf{J}$ by using the gauge-invariant condition $J_0 = \hat{\kappa} \cdot \mathbf{J}$. Note that Eq. (28) is not free of ambiguities since for the off-shell kinematics $W_\gamma \neq W_\pi$, the transformation defined by replacing S_γ by S_π and W_γ by W_π is also justified. In the energy region we are considering, the differences are negligible. We use Eq. (28) in our calculations.

To simplify numerical calculations, the collision energy W in Eq. (28) is chosen by using the fixed-scatterer approximation [20]:

$$W = \{[k_A + e(-\mathbf{k}_A/A)]^2 - (\mathbf{k}_A - \mathbf{k}_A/A)^2\}^{1/2} .$$

In a full calculation, W must depend on the Fermi momentum of the target nucleon

$$W = \{[k_A + e(\mathbf{p}_i)]^2 - (\mathbf{k}_A + \mathbf{p}_i)^2\}^{1/2} .$$

This will increase considerably the computation time since within the NBL model the πN scattering matrix in the final-state interaction term in Eq. (2) has to be computed for each initial nucleon momentum $\mathbf{p}_i$. Such a full calculation is still beyond our computation capability.

To calculate the amplitude Eq. (22), it is more convenient to expand the pion wave function χ_π and nucleon wave function ψ_α into partial waves

$$\chi^{(-)*}_{\mathbf{q}_A}(\mathbf{q}) = \sum_{l_\pi,m_\pi} Y^*_{l_\pi,m_\pi}(\hat{q}_A) Y_{l_\pi,m_\pi}(\hat{q}) \chi^{(-)*}_{l_\pi}(q) \ , \tag{29}$$

$$\psi_\alpha(\mathbf{p},m_s) = \sum_{m_{l_\alpha}} R_{n_\alpha l_\alpha}(p) \langle j_\alpha, m_{j_\alpha} | l_\alpha 1/2 m_{l_\alpha} m_s \rangle \times Y_{l_\alpha m_{l_\alpha}}(\hat{p}) \ .$$

The elementary pion photoproduction amplitude can be decomposed into a spin-nonflip term B_0 and a spin-flip term $\mathbf{B}_1$

$$t^{\gamma,\pi}_{m_f,m_i}(\mathbf{p}_f,\mathbf{q};\mathbf{p}_i,\mathbf{k}_A,\boldsymbol{\epsilon}_\lambda,W_A) = \langle m_f | B_0 + i\mathbf{B}_1 \cdot \boldsymbol{\sigma} | m_i \rangle \ . \tag{30}$$

Substituting the expansions Eqs. (29) and (30) into Eq. (22), we obtain the following partial-wave form of the pion photoproduction amplitude:

$$T_{fi} = \sum_{l_\pi m_\pi} Y^*_{l_\pi m_\pi}(\hat{q}_A) \sum_{J,M,L,S,\alpha,\beta} A^{\alpha,\beta}_{J(LS)} \int d\mathbf{p}_i d\mathbf{q} \chi^{(-)*}_{l_\pi}(q) Y_{l_\pi m_\pi}(\hat{q}) (-1)^{S+l_\alpha} \sqrt{2/[J]} i^S R_\alpha(p_f) R_\beta(p_i) \times \{[Y_{l_\alpha}(\hat{p}_f) \otimes Y_{l_\beta}(\hat{p}_i)]_{(L)} \otimes B_S\}^M_{[J]} |_{\mathbf{p}_f = -\mathbf{q}+\mathbf{p}_i+\mathbf{k}_A} \ . \tag{31}$$

We note that the basic nuclear structure input to Eq. (31) is also the one-body density matrix $A^{\alpha,\beta}_{J(LS)}$ defined in Eq. (16). This establishes the close relation between (e,e'), (π,π'), and (γ,π) reactions. The differential cross section of (γ,π) on nuclei can be calculated from the scattering amplitude Eq. (31) by using the following expression:

$$\frac{d\sigma}{d\Omega} = (2\pi)^4 \frac{q_A}{k_A} \frac{E_f(\mathbf{q}_A) E_i(\mathbf{k}_A) \omega_\pi(\mathbf{q}_A) k_A}{W_A^2} \frac{1}{2(2J_i+1)} \times \sum_\lambda \sum_{M_i,M_f} |T_{fi}|^2 \ , \tag{32}$$

where E_i and E_f are, respectively, the total energies of the initial and the final nuclear states in the ACM system. $W_A = E_i(\mathbf{k}_A) + k_A$ is the total collision energy.

The DWIA calculations defined by the above equations are carried out exactly in momentum space. All nonlocal effects due to the off-shell dynamics and nucleon recoil are included without introducing further approximations. The advantage of a momentum-space approach was emphasized in earlier (π,π') studies [6,7] and also in (γ,π) studies [10,11]. It is significantly different from the coordinate-space approach [4,8], which is derived from neglecting some, but not all, momentum dependence of the operators of Blomqvist and Laget [14] such that the Fourier transform of the momentum-space matrix elements to coordinate space can be performed analytically. To illustrate the importance of the nonlocal effects included in our approach, we will compare our full calculation with the calculation based on the factorization approximation. In the factorization approximation all relativistic transformations defined by Eqs. (23)–(26) are neglected and only the on-shell information is used to define the $\gamma N \to \pi N$ amplitude. If we express the current matrix element $\mathbf{J}$ in the usual Chew-Goldberger-Low-Nambu (CGLN) form (see Eq. (3.10) of Ref. [4]), the factorization approximation is qualitatively equivalent to making the following replacements within our momentum-space DWIA formulation:

$$\boldsymbol{\epsilon}_\lambda \cdot \mathbf{J}(\mathbf{Q},\boldsymbol{\kappa},W) \to \sum_{i=1,4} O_i(\boldsymbol{\sigma},\mathbf{q},\mathbf{k}_A,\boldsymbol{\epsilon}_\lambda) C_i(W) \ , \tag{33}$$

where C_i are scalar functions calculated from the incident photon energy in the fixed-scatterer approximation, and O_i depend on the spin operator and photon polarization vector. For example,

$$O_2 = \mathbf{k}_A \times \mathbf{q} \cdot \boldsymbol{\epsilon}_\lambda \ . \tag{34}$$

In the right-hand side of Eq. (33), the CGLN coefficients $C_i(W)$ depend only on the collision energy. This is possible only when the off-shell effect [contained in the second term of Eq. (2)] has been neglected. With this simplification, one can carry out a Fourier transform of Eq. (33) and obtain a coordinate-space formulation of DWIA. In Sec. V, we will examine the accuracy of the factorization approximation.

IV. CORE POLARIZATION

An important aspect of our calculations is to include core polarization effects in describing nuclear excitations. This is necessary since the $1p$-shell models of Cohen and Kurath [2] and Hague and Maripuu [3] were known to be inadequate in describing transitions involving collective modes, such as $E2$ transitions between states in the ground-state rotational band. In the previous (e,e') and (π,π') calculations, the procedure was to introduce effective charges or enhancement factors for those multipolarities. In this work, these effects are calculated from the polarization of the core by using the following perturbative approach:

$$\langle J_F | O_J | J_i \rangle = (J_F | O_J | J_i) + \left(J_F \left| O_J \frac{Q}{E_i - H_0} V_{\rm res} \right| J_i \right) + \left(J_F \left| V_{\rm res} \frac{Q}{E_f - H_0} O_J \right| J_i \right) \ , \tag{35}$$

where O_J is any one-body transition operator, $|J_f)$ and $|J_i)$ are initial- and final-state vectors defined in the $1p$-shell model space. The Hamiltonian H_0 represents the

mean field of the shell model. The operator Q is the projection operator onto the space outside the p-shell space. In the right-hand side of Eq. (35) the first term is the matrix element between the p-shell states, and the second and the third terms represent the effects of core polarization on the transition matrix element. The residual interaction $V_{\rm res}$ of Bertsch *et al.* [24] is used in our calculations. It is necessary to include the excitations up to $6\hbar\omega$ to get convergent results. An explicit formula of the core polarization is given in Ref. [4].

V. RESULTS FOR ^{10}B AND DISCUSSIONS

The most complex nucleus in the $1p$-shell region is ^{10}B, as discussed, for example, in Ref. [25]. A quantitative description of all of the existing data of (e,e'), (π,π'), and (γ,π) reactions on ^{10}B requires accurate treatments of both the reaction mechanisms and nuclear structure. To test our approach, it is therefore sufficient to focus on this target nucleus in this paper.

The shell model of Cohen and Kurath [2] is used to describe the excitations of ^{10}B. Following the traditional approach, we assume that the single-particle wave functions are of the oscillator form with its range parameter b [$\psi(r) \sim e^{[-(r/b)^2/2]}$] adjusted to fit the (e,e') form factors. The use of oscillator wave functions permits an exact treatment of the center-of-mass motion and simplifies considerably the calculations of nuclear matrix elements. As demonstrated in Refs. [28,29], theoretical predictions of (e,e') form factors are rather sensitive to the range parameter (b for our case) of a single-particle wave function. It is difficult to describe all of the (e,e') form factors for ^{10}B with a single value of b. In our calculations, the optimal value of b is between $b = 1.5$ and 1.6 fm. The results with $b = 1.6$ fm (solid curves) and $b = 1.5$ fm (dashed curves) are compared in Fig. 3 for the transitions to the $(J^\pi, T) = (3^+, 0)$ ground state, and in Fig. 4 for the transitions to the $(0^+, 1)$ state at 1.74 MeV and $(2^+, 1)$ state at 5.16 MeV. Note that these results are rather different from those of Ref. [28]. The (e,e') form factors are fitted in Ref. [28] by using single-particle wave functions generated from a Wood-Saxon potential and neglecting the core polarization effects. Furthermore, there are some differences in calculating the effects due to one-pion-exchange current. We see in Fig. 3 that $b = 1.6$ fm (solid curves) is favored by the ground-state $T = 0$ transition. On the other hand, Fig. 4 shows that $T = 1$ isovector transitions to the $(0^+, 1)$ and $(2^+, 1)$ excited states can be much better described by a smaller value of $b = 1.5$ fm (dashed curves). This perhaps indicates the need of a more sophisticated approach to treat either the exchange currents or core polarization effects. To illustrate this, we show in Fig. 5 the effects due to one-pion-exchange current and core polarization for the isovector $T = 1$ transitions. It is seen that both effects are very significant except in the region near zero momentum transfer. The agreement with the data at $q \sim 4$ fm region is mainly due to the core polarization effect. To

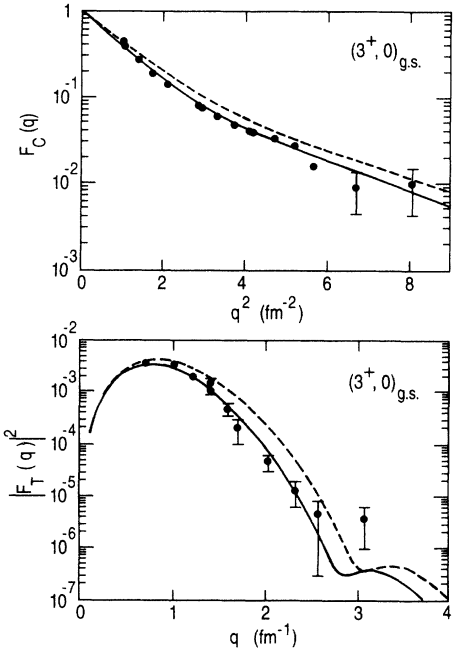

FIG. 3. The charge F_C and transverse F_T form factors of the ^{10}B ground state. Solid (dashed) curves are calculated with $b = 1.6$ (1.5) fm. Note that $F_C(0) = 1$ is chosen to normalize the data of Ref. [26]. The data of F_T are from Refs. [27,28].

fit the $T = 1$ transition form factors for these two states with $b = 1.6$, we need to have larger contributions from either one of the mechanisms or both. The possibilities are to consider short-range exchange currents and/or to use modern effective interactions to calculate the core po-

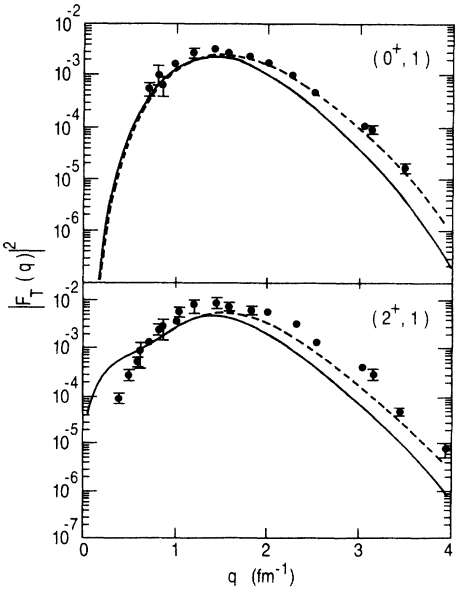

FIG. 4. The transverse form factor $F_T(q)$ for the transitions to the $(0^+, 1)$ state at 1.74 MeV and the $(2^+, 1)$ state at 5.16 MeV. The data are from Refs. [28–30]. The solid (dashed) curves are calculated with oscillator parameter $b = 1.6$ (1.5) fm.

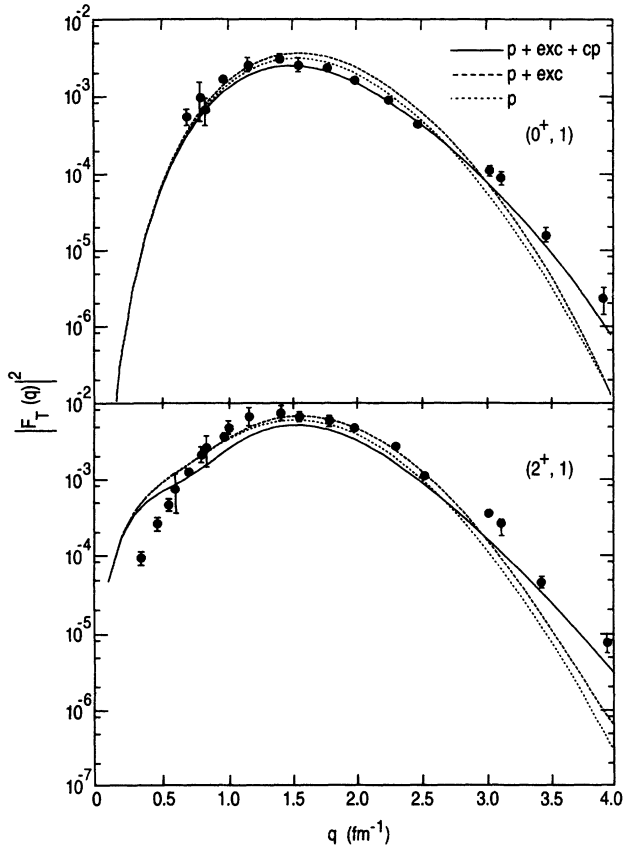

FIG. 5. The transverse form factors F_T for the transitions to the $(0^+, 1)$ state at 1.74 MeV and the $(2^+, 1)$ state at 5.16 MeV. The solid curves are results from calculations including both the one-pion-exchange current (exc) and core polarization (cp). The dashed curves are obtained when the core polarization effect is not included. The dotted curves are obtained when the one-pion-exchange current is also not included in the calculation. The data are from Refs. [28–30].

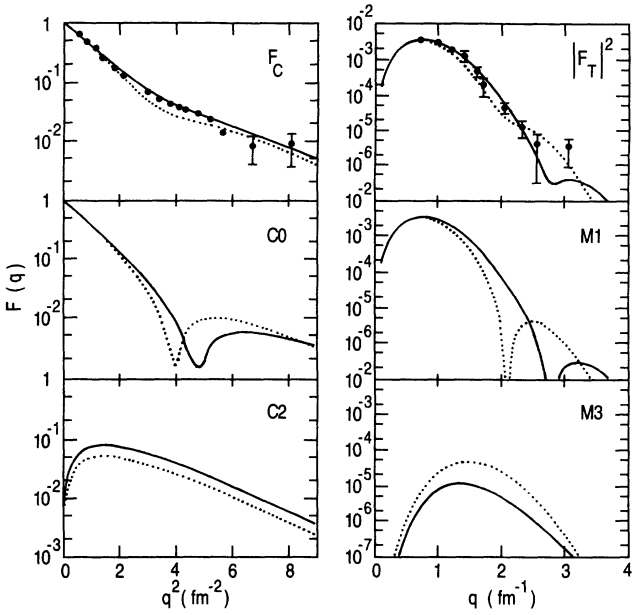

FIG. 6. The effects of core polarization on the charge F_C and transverse F_T form factors of the ^{10}B ground state. The solid curves are the results from full calculations. The dashed curves are obtained when core polarization effects are not included.

larization effects. Both are nontrivial tasks and beyond the scope of the present investigation. In the rest of the calculations based on the model of Cohen and Kurath, we will investigate results for both $b = 1.5$ and 1.6 fm.

The core polarization effects are further illustrated in Fig. 6. We show the results for the charge and transverse form factors of the ^{10}B ground state. In the top two figures of Fig. 6, it is seen that when the core polarization effects are included (solid curves), the slope of the charge form factor is better described in the region near $q^2 \sim 3$ fm^{-2}. At large momentum transfer, the shape of the transverse form factor is altered significantly by the core polarization effects. These can be understood from the lower parts of Fig. 6. It is seen that when the core polarization effects are included (solid curves), the locations of the minima of $C0$ and $M1$ form factors are shifted drastically to higher momentum transfer region. The large enhancement of the $C2$ form factor makes the static quadrupole moment in good agreement with data, while the $M3$ form factor is suppressed. An important point to mention here is that it is not possible to reproduce the effects of core polarization on form factors by introducing *state-independent* effective charges (or enhancement factors) within the $1p$-shell model space. The effects shown in Fig. 6 are the consequences of the effective interactions of Bertsch *et al.* [24]. We should emphasize here that with the core polarization effects included and the value of the oscillator constant b fixed by fitting (e,e') form factors, our subsequent (π,π') and (γ,π) calculations do not have any adjustable parameters.

Extensive (π,π') data for ^{10}B at 164 MeV were obtained by Ziedman *et al.* [31]. The data were analyzed by using the DWIA approach of Ref. [7] and the shell model of Cohen and Kurath. The fits to the data for some collective states were obtained only when enhancement factors were introduced. In this work, we will not introduce enhancement factors and also improve the calculations by (1) generating pion wave functions from the optical potential derived [22] from the Δ-hole model of pion-nucleus scattering and (2) calculating the $\pi N \rightarrow \pi N$ off-shell t matrix from the model of Nozawa, Blankleider, and Lee [1]. Furthermore, the range parameter b of the assumed oscillator single-particle wave functions has been determined in our (e,e') calculations discussed above. As comparisons, we show the results for both $b = 1.5$ and 1.6 fm. As displayed in Fig. 7, the values of b needed to obtain agreements with the data are similar to that in (e,e'). We again see that the isoscalar transition to the ground state favors $b = 1.6$ fm (solid curves), while the isovector $T = 1$ transition to the $(0^+, 1)$ state can be much better described by $b = 1.5$ fm (dashed curves). Unfortunately, the $(2^+, 1)$ state was not resolved experimentally. In Fig. 8 we show that the data in the energy region of 5.11–5.18

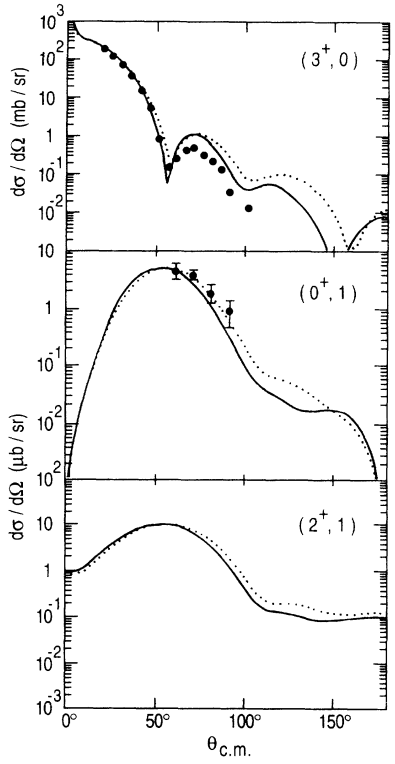

FIG. 7. The differential cross sections of pion scattering on ^{10}B leading to the $(3^+,0)$ ground state, $(0^+,1)$ at 1.74 MeV, and $(2^+,1)$ at 5.16 MeV. The solid (dotted) curves are calculated with oscillator parameter b = 1.6 (1.5) fm. The data are from Ref. [31].

MeV can be described if we add the contributions from $(2^+,1)$ (dotted curve) and also from the nearby negative parity state $(2^-,0)$ at 5.11 MeV (dashed curve). The transition density for this negative parity state is calculated by assuming a simple $(d_{5/2}, p_{3/2}^{-1})$ excitation with the strength adjusted to fit to a value of $B(E3) \sim 8e^2$ fm^6 which is close to the value < 10.4 fm^6 of Ref. [31].

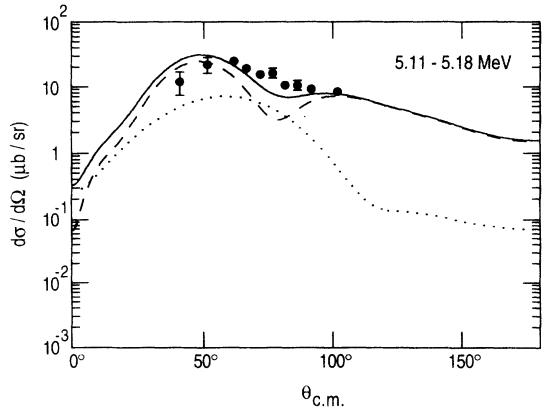

FIG. 8. The differential cross sections of pion inelastic scattering from ^{10}B leading to the $(2^+,1)$ state at 5.16 MeV (dotted curve) and the $(2^-,0)$ state at 5.11 MeV (dashed curve). The solid curve is the sum of these two contributions. The data are from Ref. [31].

The agreement with the data in these cases is certainly satisfactory. The (π,π') scattering leading to other states will be discussed later.

We now turn to presenting our results for (γ,π^+) reactions on ^{10}B. Compared with previous works [4,8–13], the main feature of our approach is to use the NBL model to generate the off-shell t matrix of the $\gamma N \to \pi N$ process to calculate the DWIA amplitude Eq. (22). Furthermore, the core polarization effects and nonlocal effects due to the target nucleon Fermi motion, as defined by Eqs. (24)–(28), are treated exactly in the calculations. The importance of these effects is illustrated in Fig. 9. The dotted curves are obtained from using the factorization approximation defined by Eq. (33) and neglecting the core polarization effects. The dashed curves are obtained when the relativistic transformations defined by Eqs. (23)–(26) are included, but the off-shell dynamics is still neglected. When the off-shell effects of the NBL model are included, the predicted cross sections are the dash-dotted curves shown in Fig. 9. A good agreement with the data of 183 MeV is obtained only when the core polarization effect is also included to obtain the solid curves. At 320 MeV, the full off-shell calculation underestimates the data by about 20% at 45° but is in good agreement with the data at 90°. Apparently, the factorization approximation Eq. (33) is not adequate for probing nuclear structure using (γ,π) reactions.

In Fig. 10, we show that the calculated (γ,π) cross sections are rather insensitive to the value of b. We use b = 1.5 fm for the rest of the results presented below.

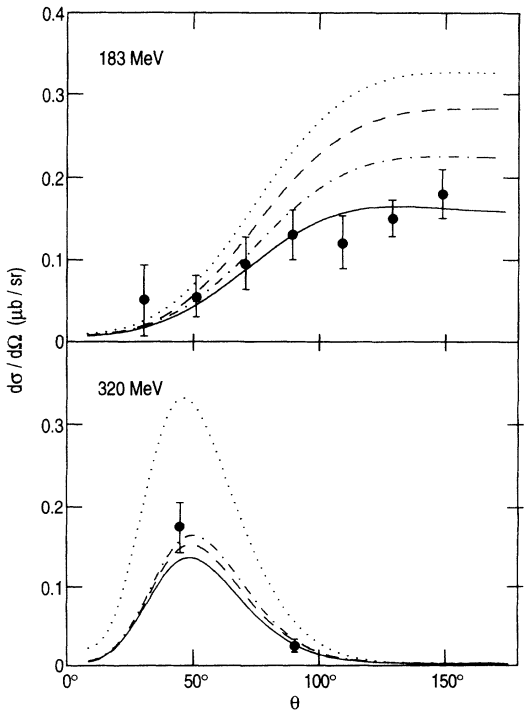

FIG. 9. The differential cross sections of the ^{10}B$(\gamma,\pi^+)^{10}$Be$(0^+,1)$ at E_γ = 183 and 320 MeV. See the text for the explanations of the curves. The data are from Refs. [32,33].

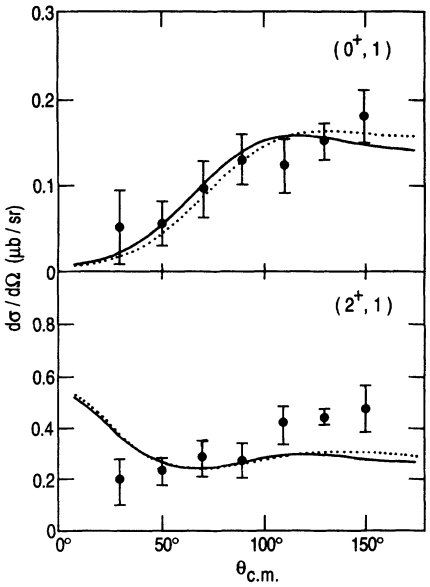

FIG. 10. The differential cross sections of the (γ,π^+) reaction on ^{10}B leading to the ^{10}Be$(0^+,1)$ state at 1.74 MeV and the ^{10}Be$(2^+,1)$ state at 5.16 MeV at E_γ = 183 MeV. The solid (dotted) curves are calculated with oscillator parameter b = 1.6 (1.5) fm. The data are from Ref. [32].

We now demonstrate that the core polarization effect is essential in obtaining a simultaneous description of (e,e'), (π,π'), and (γ,π) reactions. We first consider the cases in which the data of these three processes exist. The calculations using the shell model of Cohen and Kurath [2] are the dotted curves shown in Fig. 11. The solid curves are obtained when the core polarization effects are included. Clearly the core polarization effects improve the agreements with the data of the transitions to the $(0^+,1)$ state in all three processes. This is due to the suppression of $M3$ transition density, as seen in Fig. 6 for (e,e') transverse form factors.

In the right-hand side of Fig. 11, we see that the core polarization effect on the $(2^+,1)$ state is also significant. But it does not remove the discrepancies with the data of the (γ,π) reaction. It is therefore interesting to see whether the problem can be resolved by using a different shell model. This is done by considering the $1p$-shell model of Hauge and Maripuu [3]. The main feature of this model is that the effective interactions are deduced from nucleon-nucleon phase shifts. The model is comparable to the model of Cohen and Kurath in describing the properties of low-lying states of A = 6–14 nuclei. However, the predicted transition densities for some states can be significantly different from that of Cohen and Kurath, owing to some differences in the matrix elements of effective interactions. The comparisons of the model of Hauge and Maripuu (dotted curves) and the model of Cohen and Kurath (solid curves) are shown in Fig. 12. Their differences are small for the transitions to the $(0^+,1)$ state, but are very dramatic in all three reactions leading to the $(2^+,1)$ state. The difference mainly comes from the calculations of the $M1$ transition strengths. The results shown in Fig. 12 clearly indicate the usefulness of a consistent calculation of (e,e'), (π,π'), and (γ,π) in distinguishing theories of nuclear structure. It will be interesting to extend the measurements of ^{10}B(γ,π^+) for these two states to higher energies. To motivate these experimental efforts, we compare their energy dependences at θ = 45° and 90° in Fig. 13 for the $(0^+,1)$ state and in Fig. 14 for the $(2^+,1)$ state. We again see that their differences are very dramatic for the transition to the

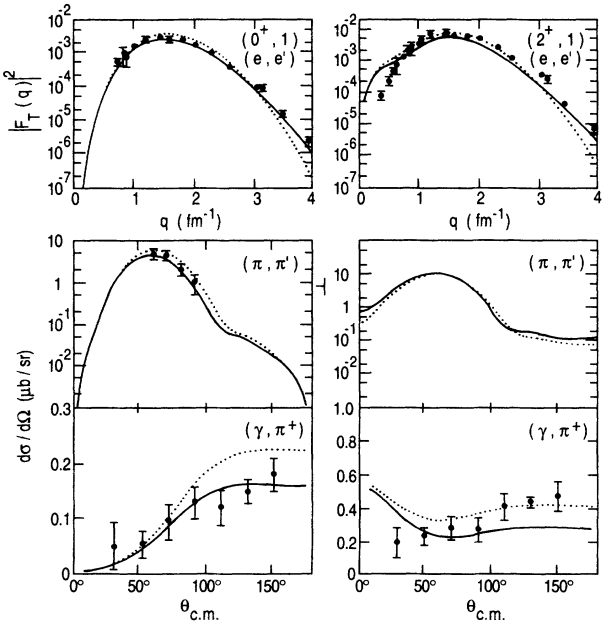

FIG. 11. The solid curves are the full calculations for (e,e') and (π,π') at E_π = 164 MeV and (γ,π^+) at E_γ = 183 MeV leading to the $(0^+,1)$ state at 1.74 MeV and the $(2^+,1)$ state at 5.16 MeV. The target nucleus is ^{10}B. The dotted curves are obtained when the effects of core polarization are neglected.

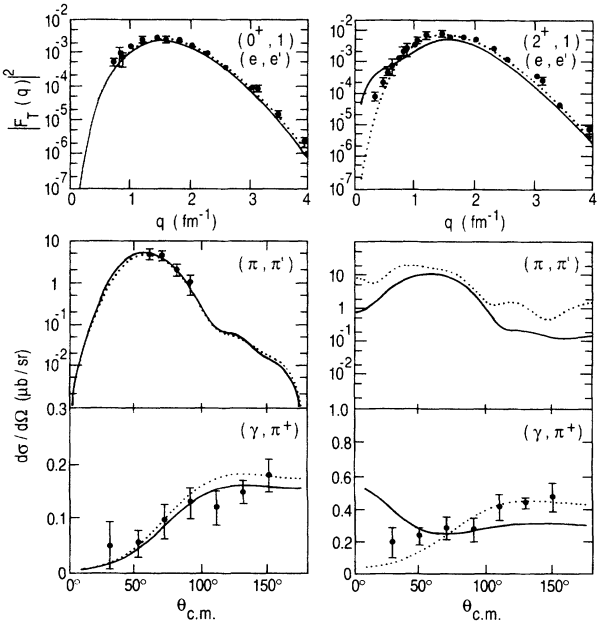

FIG. 12. The solid curves are the same as that of Fig. 11. The dotted curves are calculated from using the shell model of Hauge and Maripuu [3].

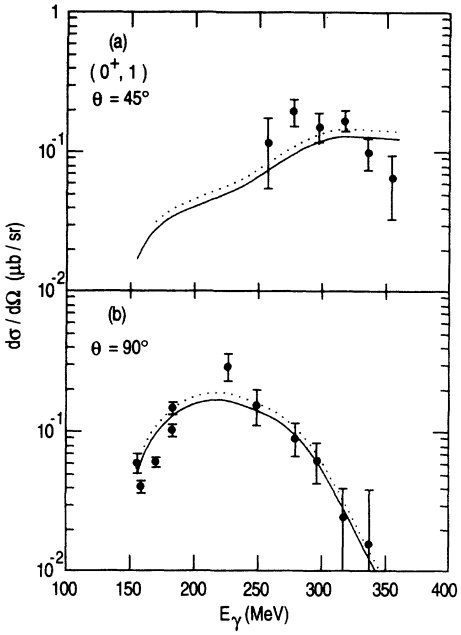

FIG. 13. The differential cross sections of $^{10}B(\gamma,\pi^+)^{10}Be(0^+,1)$ at $\theta = 45°$ and 90°. The solid (dotted) curves are calculated from using the shell model of Cohen and Kurath [2] (Hauge and Maripuu [3]). The data are from Refs. [32–35].

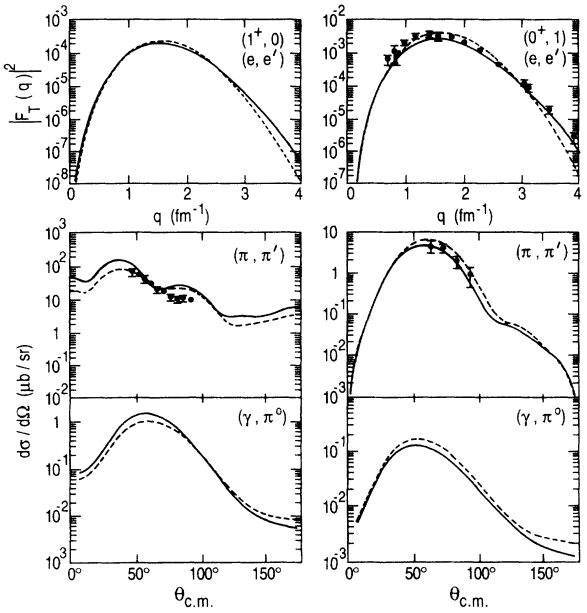

FIG. 15. The calculations for (e,e') and (π,π') at $E_\pi = 164$ MeV and (γ,π^0) at $E_\gamma = 320$ MeV leading to the $(1^+,0)$ state at 0.72 MeV and the $(0^+,1)$ state at 1.74 MeV. The solid curves are the full calculations. The dashed curves are obtained when the effects of core polarization are neglected. The (π,π') data are from Ref. [31]. The (e,e') data are from Refs. [28,29].

$(2^+,1)$ state, but are very small for the $(1^+,0)$ state.

Finally, we present predictions for future experiments in the Δ excitation energy region where extensive (π,π') data exist [31]. The results presented in Figs. 15–17 are (π,π') at $E_\pi = 164$ MeV and (γ,π^0) at $E_\gamma = 320$ MeV. For each case, the dotted curve is the prediction based on the shell model of Cohen and Kurath. The solid curve includes the effect of core polarization. All (π,π') predictions are in reasonable agreements with the data, except the case of the very weak transitions to the $(3^+,0)$ state at 4.77 MeV which has the same spin and isospin as the ^{10}B ground state. It is found [37] that, with a 1% admixture of these two states, the predicted (π,π') cross section, which is dominated by the $L = 2$

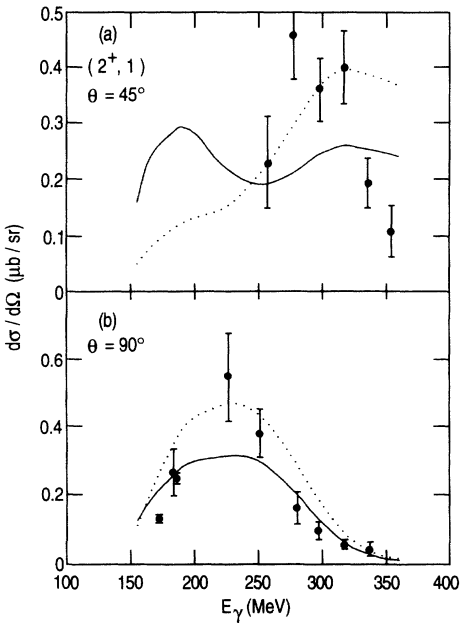

FIG. 14. Same as Fig. 13 except for the transition to the $^{10}Be(2^+1)$ state. The data are from Refs. [32–34].

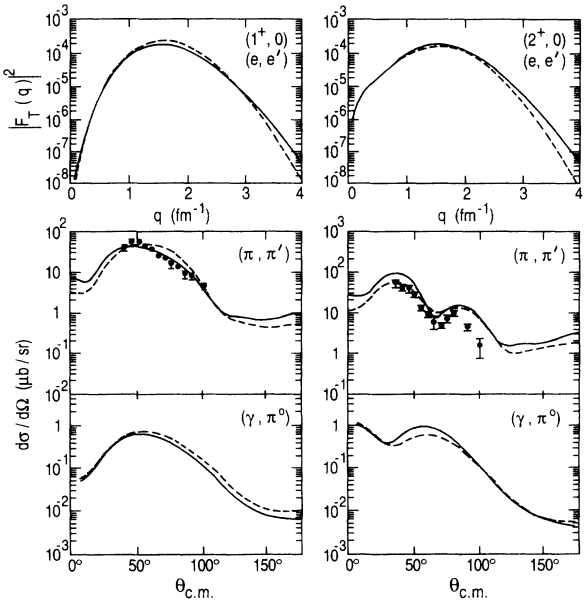

FIG. 16. Same as Fig. 15 except for the transitions to the $(1^+,0)$ state at 2.15 MeV and the $(2^+,0)$ state at 3.58 MeV.

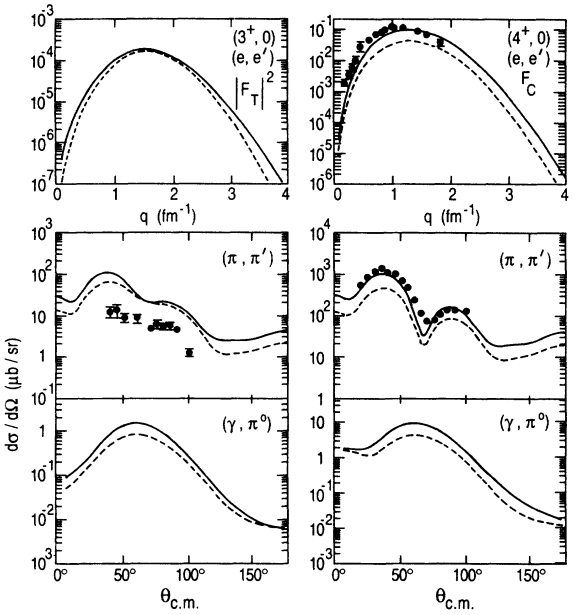

FIG. 17. Same as Fig. 15 except for the transitions to the $(3^+,0)$ state at 4.77 MeV and the $(4^+,0)$ state at 6.025 MeV. (e,e') data are from Refs. [29,36].

and $S=0$ transition, can be reduced to the experimental value while the changes in the predicted magnetic moment and the quadrupole moment of the ^{10}B ground state are negligible. To explore this point further, it will be interesting to see whether the same mixture is also needed to describe the data of (γ,π^0) data.

Another interesting case is the excitation of the $(4^+,0)$ state at 6.025 MeV shown in Fig. 17. The core polarization brings the predictions for (e,e') and (π,π') reactions to agreement with the data. An experimental test of our prediction (γ,π^0) for this state will be very interesting, since unlike introducing the enhancement factor for the (π,π') calculation in Ref. [31], the core polarization effects are calculated directly from effective interactions of Bertsch *et al.* Experimental efforts to test our predictions presented in Figs. 15–17 will complete the study of the properties of ^{10}B.

In summary, we have developed an approach to investigate the structure of nuclei by using (e,e'), (π,π'), and (γ,π) reactions. Since the (e,e') and (π,π') can be carried out by using the well-developed approaches, the focus of this work is the development of a momentum-space DWIA approach to calculate the (γ,π) cross section from the NBL model [1] of $\gamma N\to\pi N$ reaction. We have shown that the data of (e,e'), (π,π'), and (γ,π) on ^{10}B can be described consistently when core polarization is included in the structure calculations and nonlocal effects due to off-shell dynamics are accounted for rigorously. While the agreements with the data are encouraging, it is important to point out that the employed DWIA approach does not account for all of the Δ-nucleus dynamics. The use of the pion optical potential derived from the Δ-hole model [22] in our calculations at energies near the Δ excitation region certainly account for some, if not major, parts of the Δ-nucleus dynamics. But it is necessary to examine the medium effects on the Δ part of the off-shell t matrix $t^{\gamma_i\pi}$ of Eq. (22). Perhaps the information from the Δ-hole calculations of (γ,π) [23] and $(\gamma,\pi N)$ [38] reactions can be used to construct such a medium-corrected off-shell t matrix. It is, however, a nontrivial task in practice. Our investigation in this direction will be published elsewhere. Judging from the general agreements with the extensive data of ^{10}B, it is reasonable to apply our approach to carry out investigations for all $1p$-shell nuclei. Our results will be presented in the next paper.

ACKNOWLEDGMENTS

We would like to thank Dieter Kurath for informing us of his results of the excitation of the $(3^+,0)$ state at 4.77 MeV. The work was completed by the use of FACOM at the Research Center for Nuclear Physics and also SX-3 at the Computation Center Osaka University. This work was supported in part by the U.S. Department of Energy, Nuclear Physics Division, under Contract No. W-31-109-ENG-38.

[1] S. Nozawa, B. Blankleider, and T.-S. H. Lee, Nucl. Phys. **A513**, 459 (1990).
[2] S. Cohen and D. Kurath, Nucl. Phys. **73**, 1 (1965).
[3] P. S. Hauge and S. Maripuu, Phys. Rev. C **8**, 1609 (1973).
[4] T. Sato, K. Koshigiri, and H. Ohtsubo, Z. Phys. A **320**, 507 (1985).
[5] T. de Forest and J. D. Walecka, Adv. Phys. **15**, 1 (1966).
[6] T.-S. H. Lee and F. Tabakin, Nucl. Phys. **A226**, 253 (1974).
[7] T.-S. H. Lee and D. Kurath, Phys. Rev. C **21**, 293 (1980).
[8] M. K. Singham and F. Tabakin, Ann. Phys. **135**, 71 (1981).
[9] G. Toker and F. Tabakin, Phys. Rev. C **28**, 1725 (1983).
[10] L. Tiator and L. E. Wright, Phys. Rev. C **30**, 989 (1984); C. Bennhold, L. Tiator, and L. E. Wright, Can. J. Phys. **68**, 1270 (1990).
[11] R. Wittman and N. C. Mukhopadhyay, Phys. Rev. Lett. **57**, 1113 (1986).
[12] R. A. Eramzhyan, M. Gmitro, and S. S. Kamalov, Phys. Rev. C **41**, 2865 (1990).
[13] A. Nagl, V. Devanathan, and H. Überall, *Nuclear Pion Photoproduction* (Springer-Verlag, Berlin, 1991).
[14] I. Blomqvist and J. M. Laget, Nucl. Phys. **A280**, 405 (1977).
[15] K. Arita *et al.*, Phys. Rev. C **23**, 1482 (1981); K. Arita, Genshikaku kenkyu **22**, 119 (1977).
[16] A. Arima, Y. Horikawa, H. Hyuga, and T. Suzuki, Phys. Rev. Lett. **40**, 1001 (1978).
[17] K. Koshigiri, H. Ohtsubo, and M. Morita, Prog. Theor. Phys. **66**, 358 (1981).
[18] M. Fukui, K. Koshigiri, T. Sato, H. Ohtsubo, and M. Morita, Prog. Theor. Phys. **70**, 827 (1983).

[19] J. P. Elliott, A. D. Jackson, H. A. Mavromatis, E. A. Sanderson, and B. Singh, Nucl. Phys. **A121**, 241 (1968).
[20] R. H. Landau, S. C. Phatak, and F. Tabakin, Ann. Phys. **78**, 299 (1973).
[21] J. A. Carr, H. McManus, and K. Stricker-Bauer, Phys. Rev. C **25**, 952 (1982).
[22] B. Karaoglu and E. J. Moniz, Phys. Rev. C **33**, 974 (1986).
[23] J. H. Koch and E. J. Moniz, Phys. Rev. C **27**, 751 (1983); T. Takaki, T. Suzuki, and J. H. Koch, Nucl. Phys. **A443**, 570 (1985).
[24] G. Bertsch *et al.*, Nucl. Phys. **A284**, 399 (1977).
[25] D. Kurath, Nucl. Phys. **A317**, 175 (1979).
[26] T. Stovall, J. Goldemberg, and D. B. Isabelle, Nucl. Phys. **86**, 225 (1966).
[27] R. E. Rand, R. Frosch, and M. R. Yearian, Phys. Rev. **144**, 859 (1966).
[28] R. S. Hicks *et al.*, Phys. Rev. Lett. **60**, 905 (1988).
[29] E. J. Ansaldo, J. C. Bergstrom, R. Yen, and H. S. Caplan, Nucl. Phys. **A322**, 237 (1979).
[30] L. W. Fagg, R. A. Lindgren, W. L. Bendel, and E. C. Jones, Jr., Phys. Rev. C **14**, 1727 (1976).
[31] B. Ziedman *et al.*, Phys. Rev. C **38**, 2251 (1988).
[32] M. Yamazaki, K. Shoda, M. Torikoshi, O. Sasaki, and H. Tsubota, Phys. Rev. C **34**, 1123 (1986).
[33] P. E. Bosted, K. I. Blomqvist, A. M. Bernstein, S. A. Dytman, and R. A. Miskimen, Phys. Rev. Lett. **45**, 1544 (1980).
[34] D. Rowley *et al.*, Phys. Rev. C **25**, 2652 (1982).
[35] B. W. Zulkoskey, R. M. Sealock, H. S. Caplan, and J. C. Bergstrom, Phys. Rev. C **26**, 1610 (1982).
[36] E. Spamer, Z. Phys. **191**, 24 (1966).
[37] D. Kurath (private communication).
[38] T. Sato and T. Takai, Nucl. Phys. **A562**, 673 (1993).